# Assessment of THOR-50M Thoracic Injury Criteria by Population-based Accident Reconstructions

Jonas Östh, Max Nylund, Nils Olofsson, Johan Iraeus, Lotta Jakobsson

***Abstract*** Several thoracic Injury Criteria (IC) and Injury Risk Functions (IRFs) have been proposed to relate THOR-50M chest deflections to the risk of rib fracture based on post mortem human subject tests. This study assessed the IC $R_{max}$, PCScore, $D_{max}$, DcTHOR, $TIC_{NFR}$ and $TIC_{NSFR}$ and their associated IRFs for their ability to predict the rib fracture risk of human occupants in stochastic population-based frontal impact accident reconstructions based on data from NASS/CDS. A THOR-50M finite element model was positioned in an occupant compartment model parameterised with respect to its interior geometry and restraint configuration. In addition, crash pulse characteristics and restraint activation times were parameterised, and 1,000 stochastic simulations were run. For the evaluated IC, the IRF values from each simulation were aggregated to a continuous curve with respect to delta velocity (ΔV). In general, the evaluated ICs and their IRFs overpredicted the risk of injury compared with rib fracture risk curves from the real-world crash data, except $TIC_{NSFR}$ which was found to be too insensitive. The criterion that best matched the real-world crash data was PCScore, which had the closest match to the real-world data for the velocity at which 0.5 probability of AIS3+ rib fracture risk was predicted.

***Keywords*** Accident reconstruction, frontal impact, real-world crash data, rib fracture, thoracic injury criteria.

## I. INTRODUCTION

Injury Criteria (IC) and associated Injury Risk Functions (IRFs) are developed to relate a measurable physical parameter with the risk of a specific injury [1]. They can be developed through paired testing with Post Mortem Human Subjects (PMHSs) and Anthropomorphic Tests Devices (ATDs) [2–5]. Both the PMHSs and the ATDs are then subjected to as identical test conditions as possible, and the injury outcome in the PMHSs, for example the Number of Fractured Ribs (NFR), are recorded and compared with a metric, the IC, recorded in the ATD, for instance the resultant chest deflection ($R_{max}$). This has been done in the studies cited above [2–5] to create thoracic IC and IRFs for the 50$^{th}$ percentile male Test Device for Human Occupant Restraint (THOR-50M), which is the most advanced ATD for frontal impact testing developed to date [6].

A challenge for the authors who have created thoracic IRFs for the THOR-50M is the definition of the Abbreviated Injury Scale (AIS) for thoracic injury, which has changed over the years. Some the studies [3, 5] have used the AIS 2008 update [7] definition, which stipulates that three or more rib fractures, including costal cartilage fractures, are defined as a serious, level 3, or more (AIS3+) injury, while others [2, 4] preferred to create IRFs based on the NFR. However, all of the studies [2–5] have used rib fractures as the injury for which their thoracic IC and IRFs are created based on. To further complicate matters, for occupants in in real-world crashes, the NFR detected in a clinical setting with Computed Tomography (CT) or X-ray in diagnosis of injured occupants has been shown to be less frequent than from autopsy after laboratory testing in PMHS test studies [8–9]. For this reason, the Thoracic Injury Criterion (TIC) [4] was proposed for both NFR and Number of Separated Fractured Ribs (NSFR), of which the latter should better correlate to the rib fractures which can be diagnosed and detected clinically [10].

Even though the THOR-50M has a more biofidelic thorax response than the predecessor Hybrid III [6], there is no consensus about the ability of the THOR-50M to predict the risk of thoracic injury in vehicle tests. In a study that carried out 35 Offset Deformable Barrier (ODB) crash tests with the THOR-50M in the driver seat and compared with the injury outcome in 57 comparable real-world crashes in matched vehicles [11], it was found

J. Östh, PhD, (e-mail: jonas.osth@volvocars.com, tel: +46 728 88 91 72), is a Technical Expert for Human Body Modelling, M. Nylund and N. Olofsson are Safety Analysis CAE Engineers and L. Jakobsson, PhD, is a Senior Technical Leader at the Volvo Cars Safety Centre, Gothenburg, Sweden. J. Iraeus, PhD, is a Senior Researcher, J Östh an Adjunct Associate Professor and L. Jakobsson an Adjunct Professor at Chalmers University of Technology, Sweden. All authors are associated with SAFER – Vehicle and Traffic Safety Centre at Chalmers in Sweden.

that $R_{max}$ was inversely related to the injury odds; that is a 4 mm increase in $R_{max}$ led to a reduction in the injury odds. The authors [11] suggested that this discrepancy might be due to the THOR-50M not being able to adequately capture the effect of combined airbag and seat belt loading.

Using crash tests to validate ATD's IC and IRFs has its benefits in that it reproduces the conditions for which the ATD will be used closely but is limited in that physical crash tests are costly to perform, limiting the conditions that can be evaluated [11]. This can be overcome using computer aided engineering in the form of Finite Element (FE) crash simulations. This was attempted by [12] who generated alternative $R_{max}$ and PCScore IRFs for elderly occupants for the THOR-50M, by pairing it with an HBM in frontal impact sled simulations. Another simulation-based method for validation of rib fracture prediction in FE crash simulation was developed by [13] who created a generic occupant compartment model based on 14 car models tested in the New Car Assessment Programme (NCAP). The interior geometry, restraint parameters and crash pulse were parametrised using published distribution data, reverse engineering of NCAP results and Event Data Recorder (EDR) data. The parameterised occupant compartment model was used in 1,000 simulations to compare the predicted rib fracture risk of a Human Body Model to AIS3+ (AIS 2008) rib fracture risk of occupants in real-world frontal crashes.

The aim of this study was to carry out an evaluation of proposed thoracic IC and associated IRFs for the THOR-50M, for their ability to predict the risk of thoracic injury in real-world crashes, using a FE population-based accident reconstruction simulation method.

## II. METHODS

Population-based accident reconstructions were carried out according to the method developed by [13], consisting of stochastic simulations in a generic FE occupant compartment model with crash pulses parameterised from EDR data and comparison with AIS3+ (AIS 2008) rib fracture injury risk curves from the National Automotive Sampling System (NASS)/Crashworthiness Data System (CDS).

### *THOR-50M FE Model*

A FE THOR-50M Standard Build Level B (SBL-B) ATD (USNCAP version 1.7, Humanetics, Farmington Hills, MI, USA) was used for this study. This FE model of the THOR-50M is widely used by automotive manufacturers for vehicle design and the validity of the model with respect to the physical THOR-50M has been corroborated in detail for all components, subsystems and the whole ATD [14].

The ATD was positioned in the seat model 20 mm upward from the H-point location used for the HBM [13], with the legs positioned symmetrically with 270 mm width from the outer surfaces of the knee joint clevises. The feet were positioned on the floorboard, the arms close to the torso with the hands close to the steering wheel at 2 and 10 o'clock, Fig. 1 and Fig. 2. The pelvis angle of the ATD was 33°, the lumbar spine pitch adjustment 9° (slouched position), the neck pitch change adjustment 0° (neutral position) and the resulting head angles around the X and Y axes were 0°.

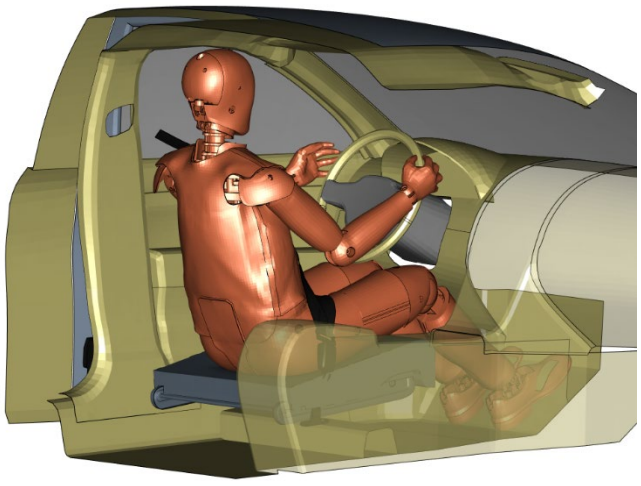

Fig. 1. THOR-50M FE model in the parameterised generic FE occupant compartment model.

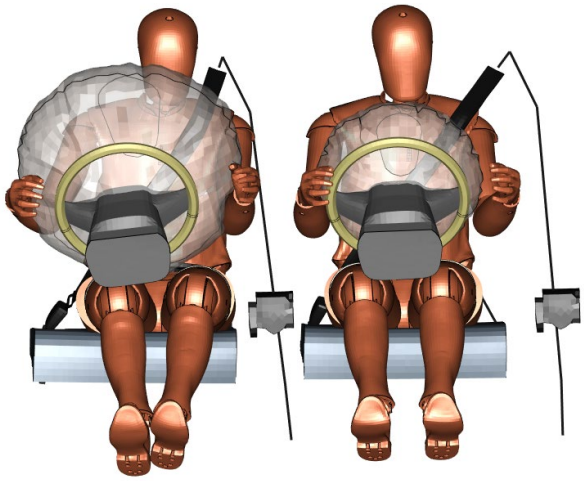

Fig. 2. The largest airbag (radius = 382 mm) and the smallest (radius = 280 mm) at 80 ms into the simulations.

The resultant chest deflections and Y and Z-axis rotations of the THOR-50M's four Infra-red Telescopic Rods for the Assessment of Chest Compression (IR-TRACCs) were evaluated using a Channel Filter Class (CFC) 180 filter in accordance with SAE J211-1 [15] and as specified by [5]. The abdomen IR-TRACCS were measured and processed similarly as the chest IR-TRACCS, to allow detection of submarining if the lap belt should enter the abdomen. Additionally, the head acceleration was measured, filtered with a CFC1000 filter, and $HIC_{15}$ [5] was calculated based on the resultant acceleration, to monitor the occurrence of hard head impacts. The simulation results were extracted using the FE post-processor META v21.0.1 (BETA CAE Systems, Luzern, Switzerland).

***Generic FE Occupant Compartment Model***

A generic occupant compartment FE model, Fig. 1, based on surfaces of 14 representative vehicles with a curb weight range from 1,100–2,000 kg [13], was used. The model was parameterised, Table AI in Appendix A, both with respect to the interior geometry (side structure distance, instrument panel distance, steering wheel height adjustment), and the restraint systems properties, Fig. 2, (restraint activation time, airbag radius and pressure, belt pre-tension, belt load limit, steering column force, steering rim force, and instrument panel stiffness).

Crash pulses were created based on Event Data Recorder (EDR) data [16] and were parameterised for the change in velocity (ΔV), Principle Direction of Force (PDOF), duration, eigenvector shape, and yaw direction, Fig. 3 and Fig. 4. Furthermore, instrument panel and foot well intrusions were parameterised and modelled.

In the present study, a total of 1,000 stochastic simulations with parameters from the distributions in Table AI in Appendix A were created, similar to the distributions used in the original study [13]. The sampling was made in LS-OPT v7.0 (ANSYS/LST, Livermore, CA) for each parameter independently using a Monte Carlo randomisation with a Latin Hypercube algorithm to ensure that extreme values were included also. Relative to the original study [13], the log-normal distribution for the restraint activation time was truncated to the interval 5–40 ms to ensure deployment of the airbag before ATD interaction with the interior in all simulations, and the steering column stroke remained constant at 90 mm.

After the parameter sampling in LS-OPT, the occupant compartment model was morphed in ANSA v21.0.1 (BETA CAE Systems, Luzern, Switzerland) to the shape determined by the geometric parameters, and the rest of the parameters were written to the input deck for simulation in LS-DYNA MPP R7.1.3 (SVN 116368, ANSYS/LST, Livermore, CA).

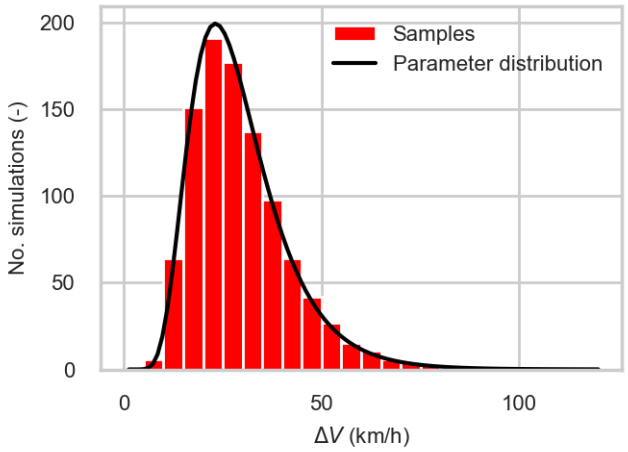


Fig. 3. ΔV histogram in the population-based accident reconstructions.

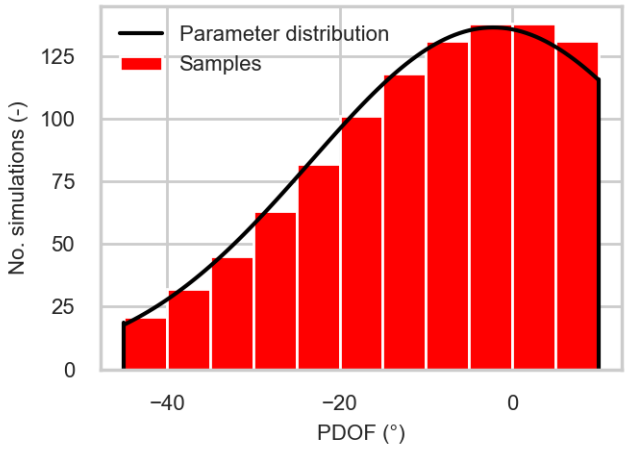


Fig. 4. Principal Direction of Force (PDOF) histogram in the population-based accident reconstructions. Negative angles indicate outboard angled impacts and positive inboard angled impacts.

***Thoracic Injury Criteria***

For each simulation, thoracic IC and associated IRFs, Table I, were calculated for an occupant age of 40 years. $R_{max}$ was calculated as the max resultant chest deflection of any of the four IR-TRACCs – the max of the Upper Left (UL), Upper Right (UR), Lower Left (LL) and Lower Right (LR) IR-TRACC. The resultant X-displacements ($D_{max}$) were calculated based on the resultant deflections and IR-TRACC rotations in accordance with the manufacturer's manual [17].

TABLE I
EVALUATED THORACIC IC AND IRFS [2–5] FOR THE THOR-50M FOR AN OCCUPANT AGE OF 40 YEARS. IARV = INJURY ASSESSMENT REFERENCE VALUE AT 50% RISK.

| IC | Calculation | IRF | IARV | Injury Level | Reference |
|---|---|---|---|---|---|
| $R_{max}$ | $\max(UL, UR, LL, LR)$ | $1 - e^{-(\frac{R_{max}}{58.183})^{2.977}}$ | 51.5 mm | AIS3+ (AIS2008) | [5] |
| *PCScore* | $\frac{UP_{tot}}{35.88} + \frac{LOW_{tot}}{29.95} + \frac{UP_{dif}}{19.5} + \frac{LOW_{dif}}{23.54}$ ,[a] | $1 - e^{-(\frac{PCScore}{8.568})^{3.31}}$ | 7.01 | AIS3+ (AIS2008) | [3] |
| $D_{max}$ | $\max(UL_x, UR_x, LL_x, LR_x)$ | $0.5(1 + \mathrm{erf}\left(\frac{\ln(D_{max}) - 3.876}{0.4351}\right))$ | 47.5 mm | NFR5+ | [2] |
| *DcTHOR* | $D_m + dD_{up} + dD_{lw}$[b] | $0.5(1 + \mathrm{erf}\left(\frac{\ln(DcTHOR) - 3.769}{0.580}\right))$ | 41.5 mm | NFR5+ | [2] |
| $TIC_{NFR}$ | $R_{max} + 1.66UP_{dif} - 1.18 * 5$,[a,c] | $1 - e^{-(\frac{TIC_{NFR}}{105.7})^{3.25}}$ | 94.2 mm | NFR3+ | [4] |
| $TIC_{NSFR}$ | $R_{max} + 3.0UP_{dif} - 2.86 * 5$,[a,c] | $1 - e^{-(\frac{TIC_{NFSR}}{181.4})^{4.79}}$ | 168.1 mm | NSFR3+ | [4] |

[a] $UP_{tot} = \max(UL + UR)$, $LOW_{tot} = \max(LL + LR)$, $UP_{dif} = \max(|UR - UL|)$,$UP_{dif} = \max(|UR - UL|)$

[b] $dD_{up}$ = $|UL_x\text{-}UR_x|_{max} - 20$; =0 if $|UL_x\text{-}UR_x| \leq 20$ or $\min(|UL_x|_{max}, |UR_x|_{max}) \leq 5$, $dD_{lw}$ = $|LL_x\text{-}LR_x|_{max} - 20$; =0 if $|LL_x\text{-}LR_x| \leq 20$ or $\min(|LL_x|_{max}, |LR_x|_{max}) \leq 5$

[c] The TIC criteria are adjusted from an age of 45 years (here 5=45−40) in the IC calculation and not in the IRF [4].

***Real-World Crash Data and Comparison to Aggregated IRF Curves***

AIS3+ (AIS 2008) rib fracture injury risk curves were generated from belted drivers (SEATPOS = 11) in frontal impacts (GAD1 = F) with deployed airbags in NASS/CDS for vehicles of model year 2000 and later, which occurred 2000–2012. Co-linear and near-side oblique frontal impacts were included by restriction of the Principle Direction of Force (315° < PDOF < 360° or PDOF < 11°). All cases which included a rollover (ROLLOVER > 0) were excluded. The analysis [13] gave a total of 5,083 cases, for which 120 occupants sustained AIS3+ (AIS 2008) rib fracture injuries, and injury risk curves with respect to $\Delta V_{Winsmash}$ were created by logistic regression.

To enable a comparison of the results from the simulations to this set of NASS/CDS data, a quasi-binominal regression model which can use the Poisson-binominal response [13] from the evaluated IRFs was used to construct aggregated IRF curves as a function of ΔV for each thoracic IRF. A Generalised Linear Model (GLM), Equation (1), was used to fit the IRF values from each simulation to ΔV before transforming it to the log-odds space through the inverse logit function, Equation (2).

$$y = C_0 + C_1 \Delta V \tag{1}$$

$$p(IRF|\Delta V) = p(IRF|y(\Delta V)) = \frac{e^{C_0 + C_1 \Delta V}}{1 + e^{C_0 + C_1 \Delta V}} \tag{2}$$

Furthermore, to enable comparison with the NASS/CDS data, the same calculation was repeated with a correction for a known bias in NASS/CDS in the Winsmash estimation of ΔV [13, 18]:

$$\Delta V_{Winsmash} = 0.81\Delta V + N(0, 8.6)\ km/h \tag{3}$$

The GLM fitting was repeated 100 times with a stochastic correction according to Equation (3) and the GLM parameters were averaged before transforming to the log-odds space with Equation (2) once more.

As the sampling of the ΔV for the simulations gave a majority of crashes at a relatively low ΔV (μ=27 km/h), Fig. 3, the influence of more high severity crashes was investigated by adding another 45 crashes with a uniform distribution in the interval 60–120 km/h. The injury risk curve aggregation process was repeated with these 45 crashes added to the original 1,000 stochastic simulations, to evaluate the effect of more high severity crashes

on the aggregated curves for each IRF.

In order to address the issue of possible underprediction of rib fractures in the NASS/CDS data, a statistical simulation was done in accordance with [13], for which a 50% and 70% underprediction of rib fractures was assumed and cases were reclassified randomly based on assumptions using the underlying injury distribution [13].

Furthermore, a comparison was also made with respect to thoracic injury MAIS3+ (AIS 1998 definition) injury risk curves constructed through logistic regression of NASS/CDS cases with EDR data by [19], allowing a comparison of THOR thoracic IC and aggregated IRFs to real-world crashes without correcting the ΔV to $\Delta V_{Winsmash}$. The sampling strategy for the study [19] was similar to the strategy used in the present to generate the population-based accident reconstruction method: Frontal impacts with confirmed belted drivers older than 18 years, excluding roll-overs or multiple events, but restricted to only vehicles rated good by the Insurance Institute for Highway Safety IIHS [19].

The analysis and comparison with real-world crash data injury risk curves were done using Python 3 (Python Software Foundation).

## III. RESULTS

All 1,000 stochastic simulations except two reached normal termination. The first failed due to negative volume in the bushings which connect the shoulder assembly to the first rib, Fig. A1, and was alleviated by re-running the simulation with a 0.6 mm null shell with self-contact for the bushing solid elements. The second failed due to a hard head contact, leading to negative volume in the head rubber, but this occurred after peak thoracic IC values, so it was kept in the data set as is. The predicted peak abdomen deflections had a normal distribution with a mean of 38 mm and a max deflection for all simulations of 58 mm, below an injury assessment reference value for 10% risk of abdominal injury of 60 mm [5]. Thirty-three simulations had a $HIC_{15}$ value over 700, mostly for higher ΔV simulations. However, for none of these 33 simulations the head impact was concluded to have affected the chest deflections.

The range of resultant chest deflections in the simulations was 12–80 mm, Table II, with the largest deflection occurring for the IR-TRACC in a simulation with a ΔV of 105 km/h and a PDOF of −14°. In this simulation, the UR IR-TRACC bottomed out and reached its max deflection as the ATD interacted with the outboard side of the steering wheel rim with the right side of the chest, bottoming through the air bag. The peak resultant deflection occurred at the UR IR-TRACC in 748 simulations, at the UL IR-TRACC in 214 and at the LR in 38 and never for the LL IR-TRACC. The range of injury probabilities, Table II and Fig. 5, from the simulations were largest for $TIC_{NFR}$ from 0.00–0.97 for a $TIC_{NFR}$ from 11.8–154.7 mm.

TABLE II.
RANGE OF THORACIC IC AND IRF VALUES IN THE 1,000 SIMULATIONS. MIN. = MINIMUM. MAX = MAXIMUM.

| | $R_{max}$ (mm) | $p(R_{max})$ AIS3+ | $D_{max}$ (mm) | $p(D_{max})$ AIS3+ | DcTHOR (mm) | p(DcTHOR) NFR5+ | $TIC_{NFR}$ (mm) | $p(TIC_{NFR})$ NFR3+ | $TIC_{NSFR}$ (mm) | $p(TIC_{NSFR})$ NSFR3+ |
|---|---|---|---|---|---|---|---|---|---|---|
| *Min.* | 12.3 | 0.01 | 12.5 | 0.00 | 7.5 | 0.00 | 11.8 | 0.00 | 8.4 | 0.00 |
| *Max.* | 80.1 | 0.93 | 78.3 | 0.94 | 71.9 | 0.89 | 154.7 | 0.97 | 211.8 | 0.88 |

The GLM model fits, Table AII in Appendix A, were best for $R_{max}$ and PCscore, Fig. 5, with $R^2$ values for the GLM models of 0.583 and 0.522, Table III. For $D_{max}$, DcTHOR, and $TIC_{NFR}$ $R^2$ values below 0.4 were found, and $TIC_{NSFR}$ had a negative $R^2$. Reflecting this, the scatter of IRF values was larger for $D_{max}$ and DcTHOR, than for $R_{max}$ and PCscore, Fig. 5 and Fig. A3 in Appendix A. The vast majority of IRF values for $TIC_{NSFR}$ were close to zero or below 0.2, even for the added high severity simulations. For this reason, $TIC_{NSFR}$ was excluded from the subsequent analysis. The added high severity impacts gave more data points with higher IRF values, but these were in general below the original aggregated IRF curves, which led to a flattening of the curve and an increased ΔV for a probability of injury of 0.5.

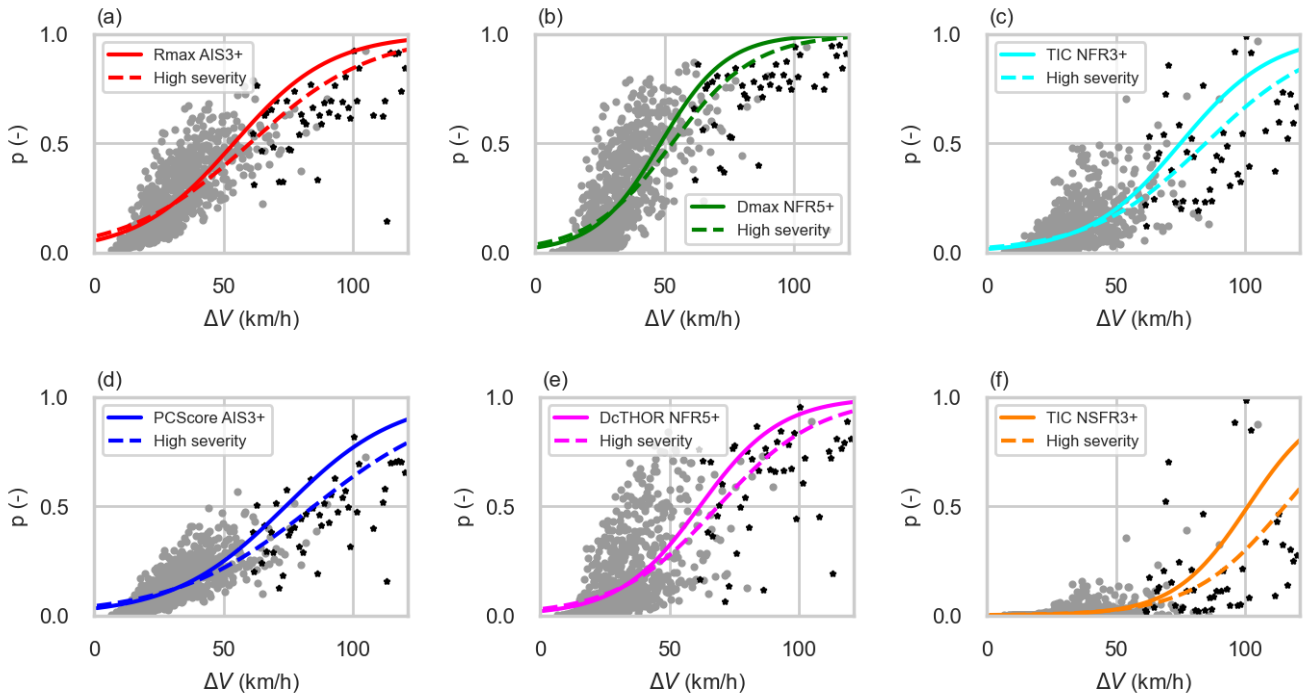


Fig. 5. Scatter plots (grey dots) for the evaluated IC and their associated IRF values vs ΔV in the 1,000 simulations and GLM aggregated IRF curves (solid lines). The black stars are the added 45 high severity crashes, and the dashed lines show the GLM aggregated IRF curves after adding them.

TABLE III.
RESULTING METRICS FOR THE AGGREGATED IRF CURVES FOR EACH IC FOR THE 1,000 SIMULATIONS, AND REAL-WORLD CRASH DATA ΔV FOR A PROBABILITY OF INJURY OF 0.5.

| | Unit | $R_{max}$ | PCSore | $D_{max}$ | DcTHOR | $TIC_{NFR}$ | $TIC_{NSFR}$ | NASS/CDS [13] | EDR data [19] | | |
|---|---|---|---|---|---|---|---|---|---|---|---|
| *Injury Level* | | AIS3+ | AIS3+ | NFR5+ | NFR5+ | NFR3+ | NSFR3+ | AIS3+ | Thoracic MAIS3+ 18-39 YO | Thoracic MAIS3+ 40-59 YO | Thoracic MAIS3+ > 60 YO |
| *ΔV(p=0.5)* | km/h | 55 | 75 | 49 | 62 | 75 | 102 | - | 99 | 85 | 70 |
| *ΔV GLM $R^2$* | - | 0.583 | 0.522 | 0.379 | 0.272 | 0.361 | -0.193 | - | - | - | - |
| *$ΔV_{Winsmash}$ (p=0.5)* | km/h | 56 | 78 | 49 | 63 | 77 | 96 | 99 | - | - | - |
| *$ΔV_{Winsmash}$ GLM $R^2$* | - | 0.451 | 0.395 | 0.229 | 0.149 | 0.233 | -0.284 | - | - | - | - |

Recalculating the aggregated IRF curves to $ΔV_{Winsmash}$, Fig. A2 in Appendix A, and comparing to the NASS/CDS data showed that all the evaluated IRFs predict higher rib fracture risk than found in the real-world crash data, Fig. 6 and Table III. The $ΔV_{Winsmash}$ for a probability for AIS3+ rib fracture of 0.5 was 99 km/h for the NASS/CDS data, while for instance it was only 55 km/h for the $R_{max}$ aggregated IRF curve.

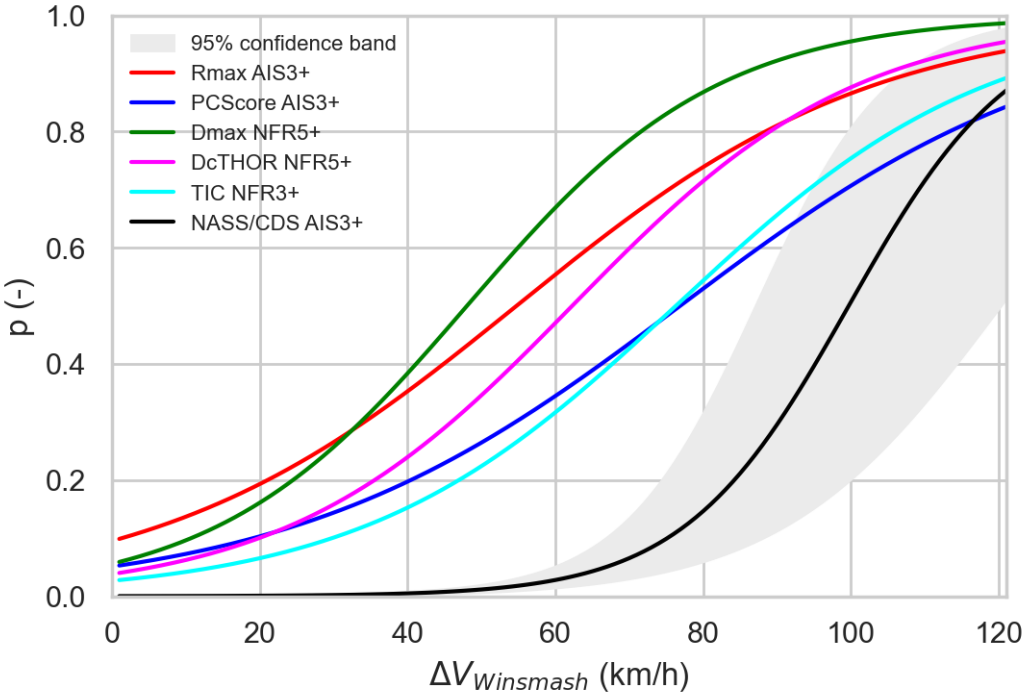


Fig. 6. Aggregated IRF curves as a function of $\Delta V_{Winsmash}$ in comparison to the risk of AIS3+ rib fracture from the NASS/CDS real-world data.

Redoing the NASS/CDS analysis for a 40 YO and assuming a 50% or 70% underprediction of AIS3+ rib fractures in NASS/CDS, Fig. 7, reduced the $\Delta V_{Winsmash}$ for a 0.5 probability of injury to 85 km/h and 64 km/h, respectively, meaning that a 70% underprediction is required for PCScore and $TIC_{NFR}$ to have higher $\Delta V_{Winsmash}$ at a probability of AIS3+ or NFR3+ of 0.5 (75 km/h for both IC). Similarly, for the thoracic MAIS3+ injury risk curves, Fig. 8, only the curve for occupants 60 years or older has a lower ΔV at 0.5 injury probability (70 km/h) than PCScore and $TIC_{NFR}$ respective aggregated IRF curve risks.

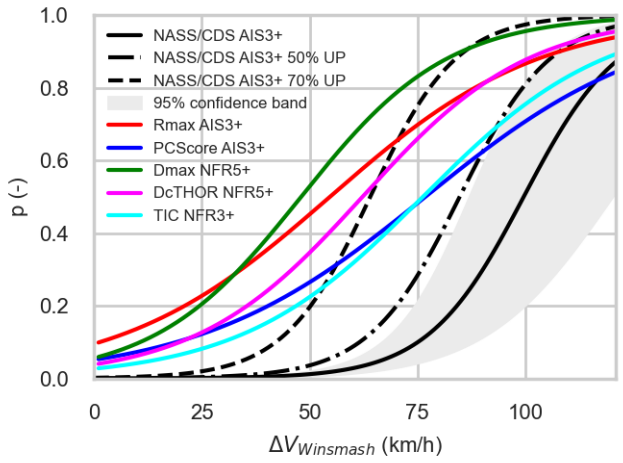


Fig. 7. Aggregated IRF curves as a function of $\Delta V_{Winsmash}$ in comparison to adjusted NASS/CDS AIS3+ rib fracture risk curves under the assumption of 50% and 70% underprediction (UP) of rib fractures in NASS/CDS [13].

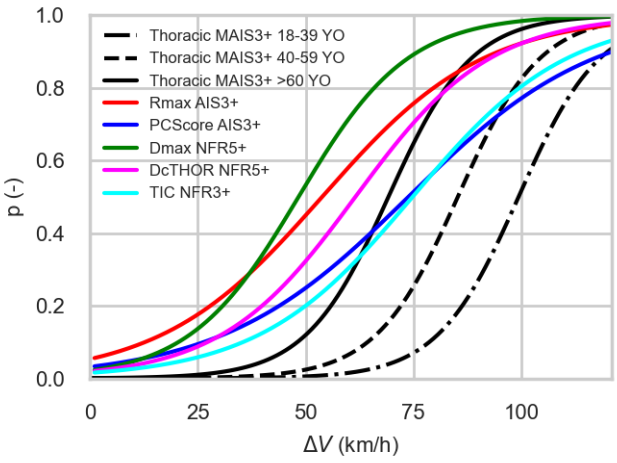


Fig. 8. Aggregated IRF curves as a function of ΔV compared with thoracic MAIS3+ risk curves vs EDR ΔV (black lines) from [19].

## IV. DISCUSSION

In this study, a stochastic, population-based accident reconstruction method was used to evaluate several proposed thoracic IC and associated IRFs for the THOR-50M. Using the FE model of the THOR worked well, with only minor fixes needed to run all the 1,000 simulations. In total, six thoracic IC and IRFs ($R_{max}$, PCScore, Dmax, DcThor, $TIC_{NFR}$, and $TIC_{NFSR}$) were calculated for each simulation and was used to fit a GLM with a coupled Poission-bionominal response, constructing aggregated IRF curves with respect to ΔV to enable comparison with occupant injury risk curves from real-world crash data analysis.

The GLM curve that best matched the real-world crash data were $R_{max}$ and PCScore, with $R^2$ values over 0.5 and aggregated IRF curves which were visually centred in the scatter of individual simulations, Fig. 5. $D_{max}$, DcTHOR and $TIC_{NFR}$ had lower $R^2$ values and also showed visually larger scatter of the individual simulation results, while $TIC_{NSFR}$ had almost all individual simulation results at low IRF risks. Even though the GLM curve fit could be computed, this curve does not really represent the aggregated risk for $TIC_{NSFR}$, but rather more the effect of fitting the GLM model to low-risk events. Therefore, $TIC_{NSFR}$ was not included in the subsequent analysis and comparison with real-world crash data.

To compare with the AIS3+ rib fracture risk from NASS/CDS, the aggregated IRF curves were recalculated to $\Delta V_{Winsmash}$ which on average is 81% of the ΔV. This recalculation and the use of the average GLM curve fit parameters flattened the aggregated IRF curves and led to a higher risk at zero $\Delta V_{Winsmash}$ than for the original ΔV curves. Nevertheless, the comparison of the aggregated IRF curves from THOR-50M to the AIS3+ rib fracture risk curve from NASS/CDS, Fig. 6, showed that all the evaluated IC and IRFs overpredicted the risk of injury for a 40 YO occupant at almost the whole range of $\Delta V_{Winsmash}$. In particular, this was the case for the range of lower velocities. For this velocity range there were a lot of crashes in the real-world data and therefore also number of simulations in the population-based simulation study, Fig. 3. The $\Delta V_{Winsmash}$ for a 0.5 probability of AIS3+ rib fracture for a 40 YO in the NASS/CDS data was 99 km/h, while for $R_{max}$ it was 56 km/h and PCScore 78 km/h for the aggregated IRF curves.

As discussed by [13], it is possible that rib fractures are underpredicted in NASS/CDS. Therefore, re-analysis of the NASS/CDS data, in which uninjured occupants were reclassified at an underprediction rate at 50% and 70%, Fig. 7, was made. This analysis showed that even for an underprediction rate of 70%, as suggested by [8], $R_{max}$, $D_{max}$, and DcTHOR would still overpredict the risk of sustaining each IC's injury at lower velocities compared to the AIS3+ rib fracture risk curve from NASS/CDS which has a probability of 0.5 at a $\Delta V_{Winsmash}$ of 64 km/h for 70% underprediction.

The evaluated ICs all have an age dependency, but for the present study the age was limited to a 40 YO occupant. Reanalysing for older occupants would shift both the aggregated IRF curves and the real-world crash data risk curves to the left in the plots vs ΔV, but would not change the conclusion that the THOR-50M IC and IRFs overpredict the risk of injury as the $\Delta V_{Winsmash}$ for a 0.5 probability of AIS3+ rib fracture in the NASS/CDS data was 72 km/h for a 70 YO occupant [13].

The evaluated ICs and IRFs are all developed based on rib fractures but are typically treated as general thoracic ICs [2–5], using rib fracture as a proxy for general thoracic injury. Therefore, occupant injury risk curves for thoracic MAIS3+ (AIS 1998 definition) as a function of ΔV rather than $\Delta V_{Winsmash}$ were also plotted for comparison to the aggregated IRF curves. The thoracic MAIS3+ injury risk curves [19], Fig. 8, do not qualitatively show any large differences with respect the NASS/CDS AIS3+ rib fracture risk curves relative to $\Delta V_{Winsmash}$ derived by [13]. For the thoracic MAIS3+ injury risk curve the ΔV for a probability of injury of 0.5 was 99 km/h and 85 km/h for occupants 18–39 YO and 40–59 YO, respectively. The observations that the THOR-50M ICs and associated IRFs are overpredicting the risk of AIS3+ rib fracture compared with the NASS/CDS data appears to be valid also for comparison to the thoracic MAIS3+ data.

In Appendix B, an attempt to alleviate the overprediction of several of the criteria is included. New $R_{max}$ Weibull parameters were found iteratively so that the GLM aggregated risk curves from the population-based accident reconstructions were fit to an interpolated thoracic MAIS3+ curve for a 40 YO vs ΔV [19]. It was possible to exactly match the aggregated GLM IRF curve from the refit $R_{max}$, but similar to the GLM fit for $TIC_{NSFR}$ the $R^2$ was negative and the resulting aggregated IRF curve was more or less just the result of the curve fitting method which is why this refit $R_{max}$ criteria should not be used. However, the iterative refitting of the $R_{max}$ IRF done in Appendix B highlights two important aspects.

The first is a potential alternative method of generating IRFs for an ATD through population-based simulations

and comparison of aggregated IRF risk to real-world crash data risk curves, which would alleviate some of the issues of using PMHSs as surrogates for live human occupants when generating IRFs. In the present study alternative combinations to $R_{max}$ was also tested (results not presented), for instance the sum of all peak resultant deflections or the mean peak resultant deflection for each IR-TRACC, but with the same poor GLM curve fit.

The second is a limitation of the deflection measurements of the THOR-50M. The stiffness of the THOR chest and rib cage has been validated with respect to human subject data [6, 20], but some of the test conditions only give up to approximately 40–50 mm skeletal deflection (4.3 m/s Kroell pendulum). The simulations carried out in the present study show a biphasic response of the THOR-50M, Fig. 9, with an approximately linear increase of peak resultant chest deflection $R_{max}$ up to around 60 km/h ΔV, and then a lower slope for higher ΔVs. At the same time, the real-world data injury risk curves, Fig. 6 and Fig. 8, indicate that for a ΔV or $\Delta V_{Winsmash}$ below 60 km/h a 40 YO occupant has a low risk of AIS3+ rib fracture or MAIS3+ thoracic injury. This means that for a 40 YO and younger occupant, the THOR-50M will be insensitive to measure chest deflections in the ΔV ranges for which rib fractures occur in real-world crashes. For older occupants, the range of ΔVs which can generate rib fractures will be lower and might overlap with the sensitive deflection range of THOR-50M. One speculation for why this is could be that the ATD has been developed using PMHS data and therefore better represent an older subject population.

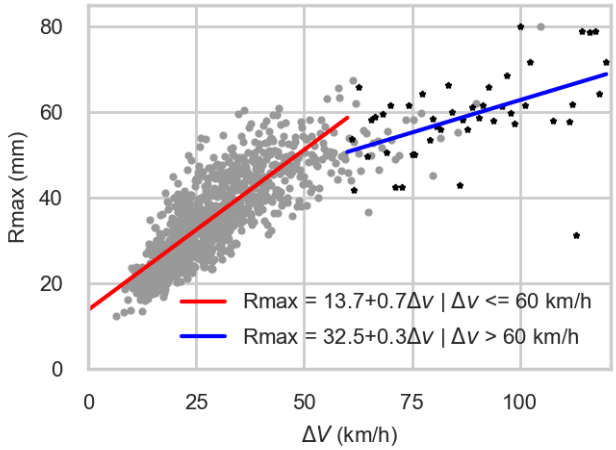


Fig. 9. Scatter plots (grey dots) of $R_{max}$ vs ΔV in the 1,000 simulations. The black stars are the added 45 high severity crashes, and the solid lines are linear curve fits for all simulations with a ΔV≤60 km/h and ΔV> 60 km/.

## V. CONCLUSIONS

A FE model of the THOR-50M was subjected to synthetic, stochastic, population-based accident reconstructions representative of a sample of crashes from NASS/CDS. For each one of the 1,000 simulations, six thoracic IC and IRF values were calculated and aggregated IRF curves for a 40 YO were generated. Of the evaluated IC, $TIC_{NSFR}$ was too insensitive and gave low IRF probabilities for almost all simulations regardless of ΔV, making it unsuitable for THOR-50M in impact severities which can be expected to generate thoracic injury. On the other hand, all the other evaluated ICs overpredicted the risk of rib fracture considerably compared with the risk of injury for an occupant based on the NASS/CDS real-world crash data. $D_{max}$ and $R_{max}$ were the most sensitive IC, predicting a probability of injury of 0.5 at a $\Delta V_{Winsmash}$ of 49 km/h and 55 km/h, respectively, while the NASS/CDS data predicted 0.5 probability of injury at 99 km/h or 64 km/h if an underprediction of 70% of AIS3+ rib fractures was assumed in NASS/CDS. In this regard, $TIC_{NFR}$ and PCScore matched the real-world crash data better, with $\Delta V_{Winsmash}$ at 0.5 injury probability of 77 and 78 km/h, respectively. Of these two criteria, PCScore is recommended to be used with THOR-50M as it had the best fit for the GLM, and hence the aggregated IRF curve better represents the underlying IRF values.

## VI. ACKNOWLEDGEMENT

This work was carried out at SAFER, Vehicle and Traffic Safety Centre at Chalmers University of Technology, Gothenburg, Sweden, and funded by FFI-Strategic Vehicle Research and Innovation, by Vinnova, the Swedish Energy Agency, the Swedish Transport Administration, and the Swedish vehicle industry.

## VII. REFERENCES


[1] Schmitt, K.-U., Niederer, P.F., Cronin, D.S., Morrison, B. III, Muser, M.H., Walz, F. (2019) *Trauma Biomechanics – An Introduction to Injury Biomechanics.* Springer Verlag, Cham, Switzerland.

[2] Davidsson, J., Caroll, J., *et al.* (2014) Development of Injury Risk Functions for use With the THORAX Demonstrator; an Updated THOR. *Proceedings of the IRCOBI Conference*, Berlin, Germany.

[3] Poplin, G.S., McMurry, T.L., *et al.* (2017) Development of Thoracic Injury Risk Functions for the THOR ATD. *Accident Analysis and Prevention* 106: 122–130.

[4] Trosseille, X., Baudrit, P. (2019) Updated Chest Injury Criterion for the THOR Dummy. *Proceedings of the ESV Conference*, Eindhoven, the Netherlands.

[5] Craig, M., Parent, D., Lee, E., Rudd, R., Takhounts, E., Hasija, V. (2020) *Injury Criteria for the THOR 50th Male ATD*. National Highway Traffic Safety Administration, Washington, DC, USA.

[6] Parent, D., Craig, M., Moorhouse, K. (2017) Biofidelity Evaluation of the THOR and Hybrid III 50$^{th}$ Percentile Male Frontal Impact Anthropomorphic Test Devices. *Stapp Car Crash Journal* 61: 227–276.

[7] Association for the Advancement of Automotive Medicine (2008) *The abbreviated injury scale-2005 revision, update 2008*. AAAM, Des Plaines, USA.

[8] Crandall, J., Kent, R., Patrie, J., Fertile, J., Martin, P. (2000) Rib Fracture Patterns and Radiologic Detection a Restraint-based Comparison. *Proceedings of the Annual AAAM Scientific Conference*, Chicago, Illinois, USA, p. 235.

[9] Schulze, C., Hoppe, H., Schweitzer, W., Schwendener, N., Grabherr, S., Jackowski, C. (2013) Rib Fractures a Postmortem Computed Tomography (PMCT) validated against Autopsy. *Forensic Science International* 233(1): 90–98.

[10] Trosseille, X., Baudrit, P., Leport, T., Vallancien, G. (2008) Rib Cage Strain Pattern as a Function of Chest Loading Configuration. *Stapp Car Crash Journal* 52: 205–231.

[11] Brumbelow, M.L., Jermakian, J.S., Arbelaez, R.A. (2022) Predicting Real-World Thoracic Injury Using THOR and Hybrid III Crash Tests. *Proceedings of the IRCOBI Conference*, Porto, Portugal.

[12] Eggers, A., Wisch, M., et al. (2019) Improved Thoracic Injury Risk Functions for the THOR-M-50 Developed in a New Simulation-based Approach. *Proceedings of the ESV Conference*, Eindhoven, the Netherlands.

[13] Iraeus, J., Lindquist, M. (2016) Development and Validation of a Generic Finite Element Vehicle Buck Model for the Analysis of Driver Rib Fractures in Rear Life Nearside Oblique Frontal Crashes. *Accident Analysis and Prevention 95*: 42–56.

[14] Humanetics (2020) *THOR-50M U.S. NCAP Dummy Model LS-DYNA Release Version 1.7 Technical Report*. Humanetics, Farmington Hills, MI, USA.

[15] Society of Automotive Engineers (2007) *SAE J211-1 Instrumentation for Impact Test, Surface Vehicle Recommended Practice*. Society of Automotive Engineers, Warrendale, PA, USA.

[16] Iraeus, J., Lindquist, M. (2014) Analysis of delta velocity and PDOF by means of collision partner and structural involvement in real life crash pulses with modern passenger cars. *Traffic Injury Prevention* 15(1): 56–65.

[17] Humanetics (2016) *USER MANUAL: 3D IR-TRACC THOR-50M*. Humanetics, Farmington Hills, MI, USA.

[18] Funk, J.R., Cormier, J.M., Gabler, H.C. (2008) Effect of Delta-V errors in NASS on Frontal Crash Risk Calculations. *Proceedings of the AAAM Conference*, San Diego, CA, USA.

[19] Brumbelow, M.L. (2019) Front Crash Injury Risks for Restrained Drivers in Good-rated Vehicles by Age, Impact Configuration, and EDR-based Delta V. *Proceedings of the IRCOBI Conference*, Florence, Italy.

[20] Parent, D.P., Craig, M., Ridella, S.A., McFadden, S.D. (2013) Thoracic Biofidelity Assessment of the THOR Mod Kit ATD. *Proceedings of the ESV Conference*, Seoul, South Korea.

## VIII. APPENDIX A

TABLE AI.

PARAMETER VARIATION AND DISTRIBUTIONS USED FOR THE POPULATION-BASED ACCIDENT RECONSTRUCTION METHOD.

| Parameter | Unit | Distribution | Distribution parameters |
|---|---|---|---|
| *Airbag size (radius)* | [mm] | Normal | μ = 332, σ = 18 |
| *Steering height adjustment rot.* | [°] | Uniform | Min. = −2.7, max. = 2.7 |
| *Side structure distance* | [mm] | Normal, truncated | μ = 0, σ = 33, min. = −60, max. = 20 |
| *Instrument panel distance* | [mm] | Normal, truncated | μ = 0, σ = 33, min. = −60, max. = 60 |
| *Delta velocity, ΔV* | [km/h] | LOG-normal | μ = 3.3, σ = 0.4 |
| *Principal direction of force* | [°] | Normal, truncated | μ = −2.2, σ = 21.2, min. = −45, max. = 10 |
| *Duration* | [ms] | Normal | μ = 109.6, σ = 16.2 |
| *Pulse eigenvector 1* | [-] | Normal | μ = −0.48+0.015ΔV, σ = 1.64 |
| *Pulse eigenvector 2* | [-] | Normal | μ = 0.97+0.03ΔV, σ = 1.05 |
| *Pulse eigenvector 3* | [-] | Normal | μ = −0.33+0.01ΔV, σ = 0.74 |
| *Yaw scale factor* | [-] | Normal | μ = −0.068, σ = 0.0019 |
| *Intrusion instrument panel* | [mm] | Exponential | Step one: Bernoulli(p = invlogit(−5.47 + 0.074ΔV)) Step two: Exponential rate = 0.079 |
| *Intrusion floor panel* | [mm] | Exponential | Step one: Bernoulli(p = invlogit(−5.15 + 0.076ΔV)) Step two: Exponential rate = 0.071 |
| *Airbag pressure scaling factor* | [-] | Normal | μ = 1.31, σ = 0.10 |
| *Restraint activation time* | [ms] | LOG-normal, truncated | μ = 3.04, σ = 0.64, min. = 5, max. = 40 |
| *Steering column force* | [kN] | Normal | μ = 4.8, σ = 0.90 |
| *Steering rim force* | [kN] | Normal | μ = 2.8, σ = 0.80 |
| *Belt pretensioner force* | [kN] | Normal | μ = 1.93, σ = 0.47 |
| *Belt force limiter* | [kN] | Normal | μ = 3.94, σ = 0.69 |
| *Knee force stiffness* | [kN/100 mm] | Normal, truncated | μ = 9.45, σ = 3.86, min. = 3, max. = 20 |
| *Belt friction* | [-] | Uniform | Min. = 0.2, max. = 0.4 |
| *Seat friction* | [-] | Uniform | Min. = 0.2, max. = 0.4 |
| *IP friction* | [-] | Uniform | Min. = 0.2, max. = 0.4 |
| *Airbag friction* | [-] | Uniform | Min. = 0.2, max. = 0.4 |
| *Door friction* | [-] | Uniform | Min. = 0.2, max. = 0.4 |
| *Buckle slipring friction* | [-] | Normal, truncated | μ = 0.18, σ = 0.08, min. = 0, max. = 0.5 |

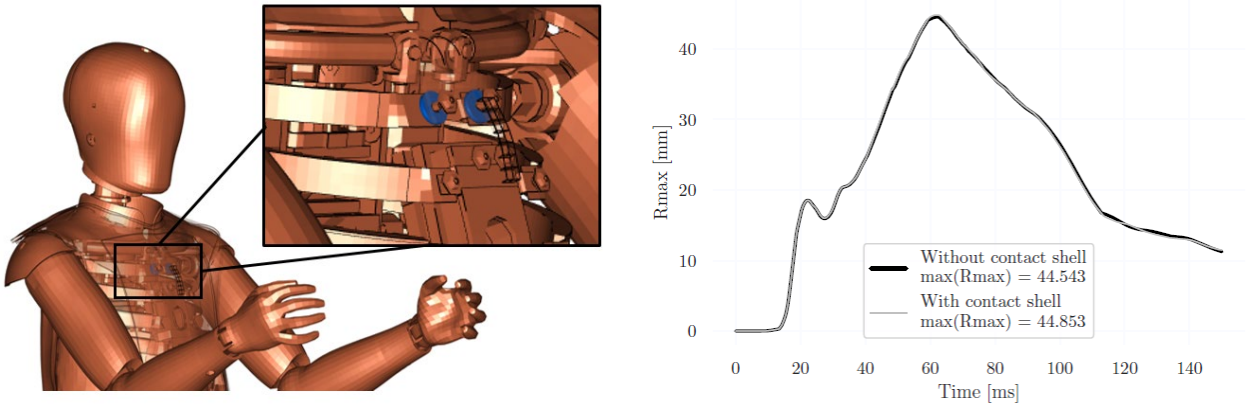


Fig. A1. Left: Chest bushings in the THOR-50M FE model which were complemented with null-shells in self-contact for one high severity impact. Right: Difference in $R_{max}$ with and without the bushing null-shells.

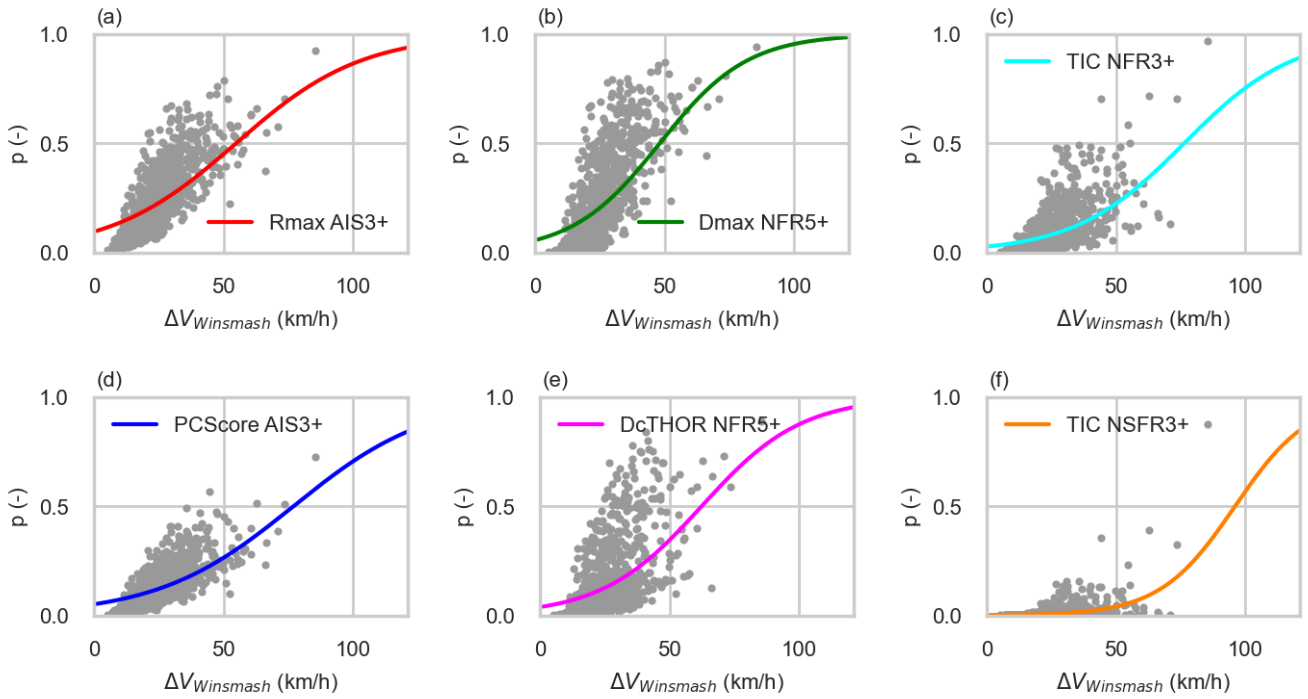


Fig. A2. Scatter plots (gray dots) for the evaluated IC and their associated IRF values vs $\Delta V_{Winsmash}$ in the 1,000 simulations and GLM aggregated IRF curves (solid lines). The Winsmash correction shifts the results to the left, flattens the GLM curves and moves the Y-axis intercept upward, compared with the ΔV plots in Fig. 5.

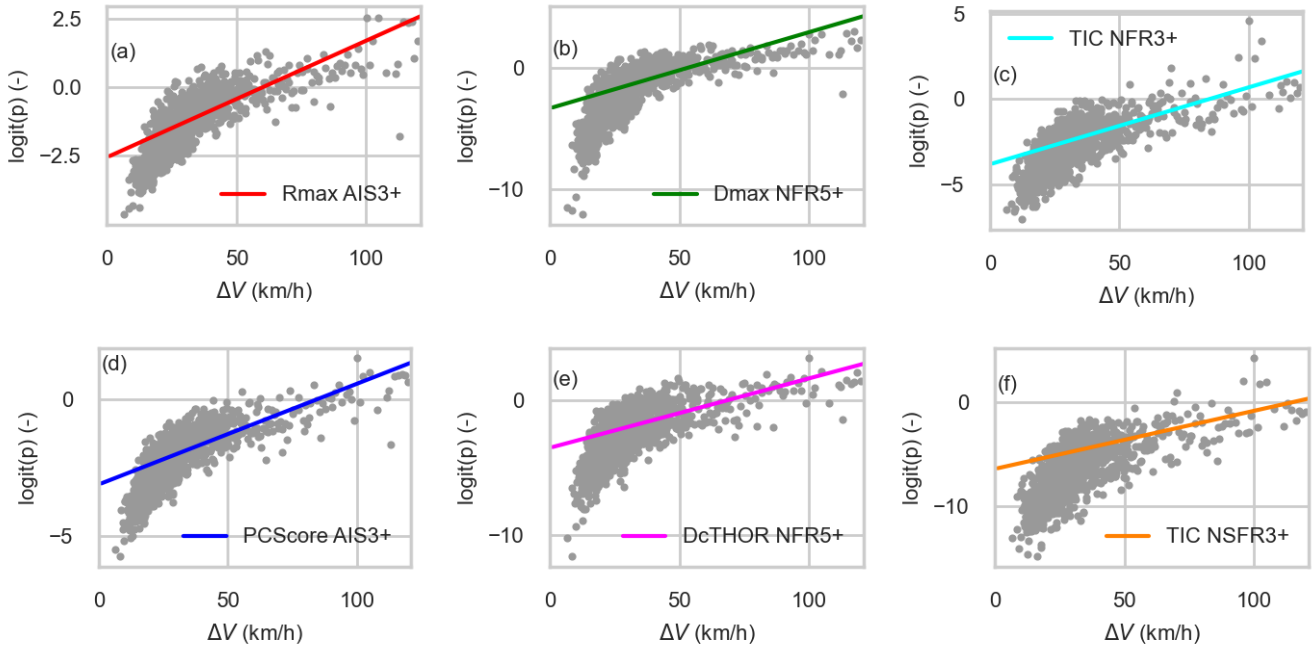


Fig. A3. Scatter plots (gray dots) for the evaluated IC and their associated IRF values vs ΔV in the 1,000 simulations and GLM aggregated IRF curves (solid lines) in the log-odds space.

TABLE AII.
GENERALIZED LINEAR MODEL (GLM) PARAMETERS.

| | Unit | $R_{max}$ | PCSore | $D_{max}$ | DcTHOR | $TIC_{NFR}$ | $TIC_{NSFR}$ |
|---|---|---|---|---|---|---|---|
| Injury Level | | AIS3+ | AIS3+ | NFR5+ | NFR5+ | NFR3+ | NSFR3+ |
| | | - | - | - | - | - | - |
| $\Delta V$ GLM $C_0$ | - | 2.88109 | 3.42088 | 3.81428 | 3.94380 | 4.18155 | 7.09584 |
| $\Delta V$ GLM $C_1$ | - | 0.05349 | 0.04631 | 0.07884 | 0.06405 | 0.05586 | 0.07027 |
| | | - | - | - | - | - | - |
| $\Delta V_{Winsmash}$ GLM $C_0$ | - | 2.25935 | 2.93409 | 2.83743 | 3.24041 | 3.61523 | 6.62417 |
| $\Delta V_{Winsmash}$ GLM $C_1$ | - | 0.04138 | 0.03836 | 0.05918 | 0.05224 | 0.04762 | 0.06968 |

## IX. APPENDIX B

An attempt was made to refit the Weibull model for $R_{max}$ [5] to a thoracic MAIS3+ risk curve for a 40 Year Old (YO) occupant interpolated from the 18–39 YO and 40–59 YO risk curves [19]. With the recorded $R_{max}$ values from the stochastic simulations, new Weibull IRF parameters were searched for so that the GLM model closely matched the target thoracic MAIS3+ risk curve.

Iteratively finding parameters for the $R_{max}$ Weibull IRF (p=1-exp(-($R_{max}$/β)^α) such that the GLM generated from the $R_{max}$ values from the 1,000 simulations resulted in a good match, Fig. B1, between the GLM aggregated IRF curve and the thoracic MAIS3+ injury risk curve for a 40 year old interpolated from [19]. The GLM curve fit, however, was poor, with negative $R^2$ of −0.897 and most IRF values close to zero. To match the real-world crash data with the method used here, a steep change in the refitted $R_{max}$ IRF (with Weibull parameters β=65.2631 and α=18.739) was needed, Fig. B2.

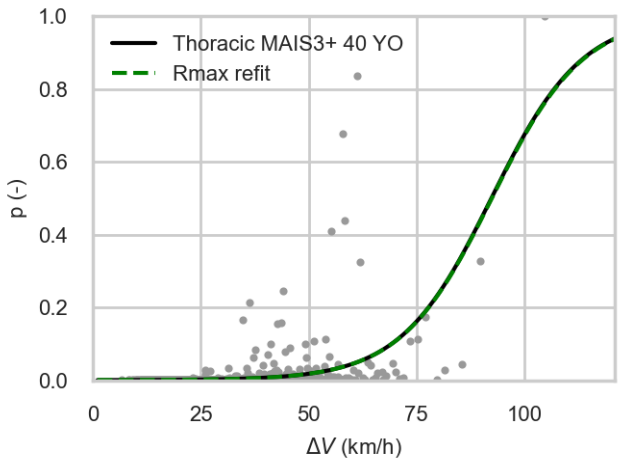


Fig. B1. Scatter (gray dots) of refitted $R_{max}$ IRF values in the 1,000 simulations and GLM aggregated IRF curve (dashed green) after iteration to find Weibull parameters, plotted on top of a thoracic MAIS3+ injury risk curve for a 40 year old (YO) occupant interpolated from [19].

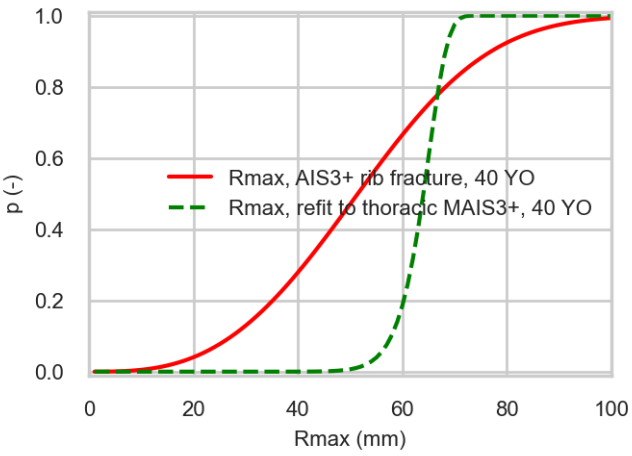


Fig. B2. $R_{max}$ IRF for AIS3+ rib fracture for a 40 year old (YO) [5] (red solid line) and refit $R_{max}$ Weibull IRF matching the curve in Fig. B1.